Appendix V:

Preparation and Catalytic Activity of Ni-Co Molybdates Supported on Alumina, Magnesia, Titania, Zirconia and Mixed Alumina-Magnesia - Detailed Results -

V. Preparation and Catalytic Activity of Ni-Co molybdates supported on alumina, magnesia, titania, zirconia and mixed alumina-magnesia

V.1 Alumina-, magnesia- and mixed Al_2O_3-MgO-dispersed catalysts prepared by impregnation and sol-gel methods

V.1.1 Characterization of the pure supports

Before describing the characteristics of the dispersed Ni(Co)-Mo-O catalysts, we will review those of the supports used from these experiments. Commercially available supports were used for the preparation of impregnated catalysts on alumina and magnesia. When the sol-gel method was applied, the corresponding pure supports were also prepared according to the same procedure to get a reference picture of the host oxide matrix, in which the molybdate phase has been dispersed.

The thermal behaviour of the precursor gels of each support has been investigated by TGA. In the case of the alumina precursor, three weight losses are observed: the first weight loss of 20 %, between 303 and 443 K can be attributed to the desorption of physically adsorbed water and organic molecules. Desorption of chemisorbed water molecules and residual organic groups occurred between 443 and 533 K and produced a weight loss of 5 %. The last weight loss of 14 % between 533 and 823 K could be produced by the dehydroxylation of the sample during the transformation of γ-boehmite into alumina according to: $2AlO(OH) \rightarrow Al_2O_3 + H_2O$ (wt. 18 %). The further gradual weight loss above 823 K is probably associated with the loss of hydroxyl groups in the structure (184).

Similarly in the thermogram of the magnesia precursor gel, the first weight loss of 12 % between 303 and 493 K is assigned to the vaporization of water and ethanol physically adsorbed on the solid. The removal of residual alkoxy groups and OH groups weakly bound to the solid occurred between 493 and 633 K, with a weight loss of 28 %. The last weight loss of 6 % between 633 and 973 K refers to the total dehydroxylation of MgO (185). The thermogram of the mixed alumina-magnesia sol-gel precursor was very similar to the previous ones.

In consequence of these results, a standard calcination temperature of 773 K for 20 hours under 1 l min^{-1} flow of dry air has been selected for all supports prepared by the sol-gel method.

In both commercial and sol-gel prepared catalysts, alumina appears as its γ-phase; and magnesia as the periclase phase (file n° 45-0946).

The textural properties of alumina-, magnesia- and alumina-magnesia were determined from complete nitrogen adsorption/desorption isotherms analyzed according to the BJH method (for the pore volume and diameter).

The surface area of a sample of Al_2O_3 prepared by the sol-gel method was found to be equal to 252 m^2 g^{-1}. The isotherm of this alumina sample exhibits a shape corresponding to type IV in Brunauer's classification; this support is characterized by a Vp equal to 0.48 cm^3 g^{-1} and a Dp of 5.4 nm. The surface area of commercial Al_2O_3 was equal to 157 m^2 g^{-1} and it displays an isotherm with a shape corresponding to type IV + II; this support is characterized by a Vp equal to 0.27 cm^3 g^{-1} and a Dp of 5.1 nm.

The surface area of sol-gel-prepared MgO was equal to 123 m^2 g^{-1}. The isotherm of MgO exhibits a shape corresponding to type II in Brunauer's classification; this support is characterized by a Vp equal to 0.47 and a pore diameter of 31 nm. The surface area of commercial MgO was equal to 1.1 m^2 g^{-1} and it displays an isotherm with a shape corresponding to type II.

The mixed Al_2O_3-MgO support prepared by the sol-gel method has a specific surface area equal to 228 m^2 g^{-1}. It is characterized by an isotherm displaying a type IV shape, with porous volume of 0.38 cm^3 g^{-1} and a pore diameter of 5.4 nm.

V.1.2 Thermal behaviour of all sol-gel precursors

Three thermograms of sol-gel precursor of Ni and Co molybdates dispersed in alumina, magnesia and mixed alumina-magnesia are given as examples in the figures V.1 to 3. For all sol-gel samples, three weight losses regions are observed exactly as for the precursors gels of the corresponding pure supports already described in section V.1.1.

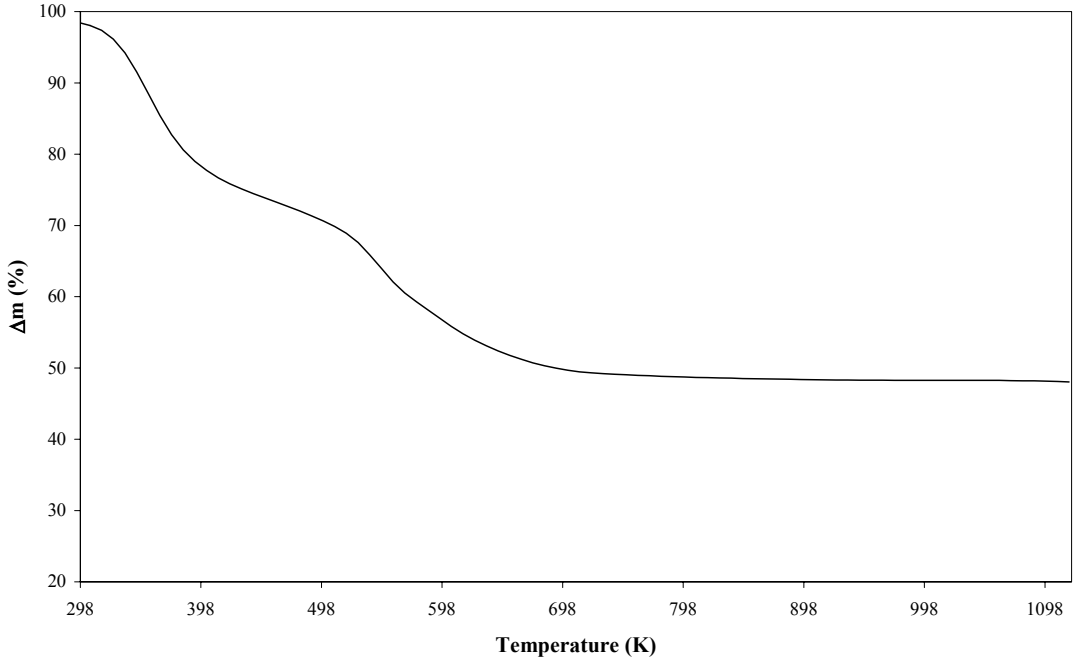

Fig.V.1: Thermogram of sol-gel precursor $NiMoO_4$ dispersed on alumina (Al/Mo = 5).

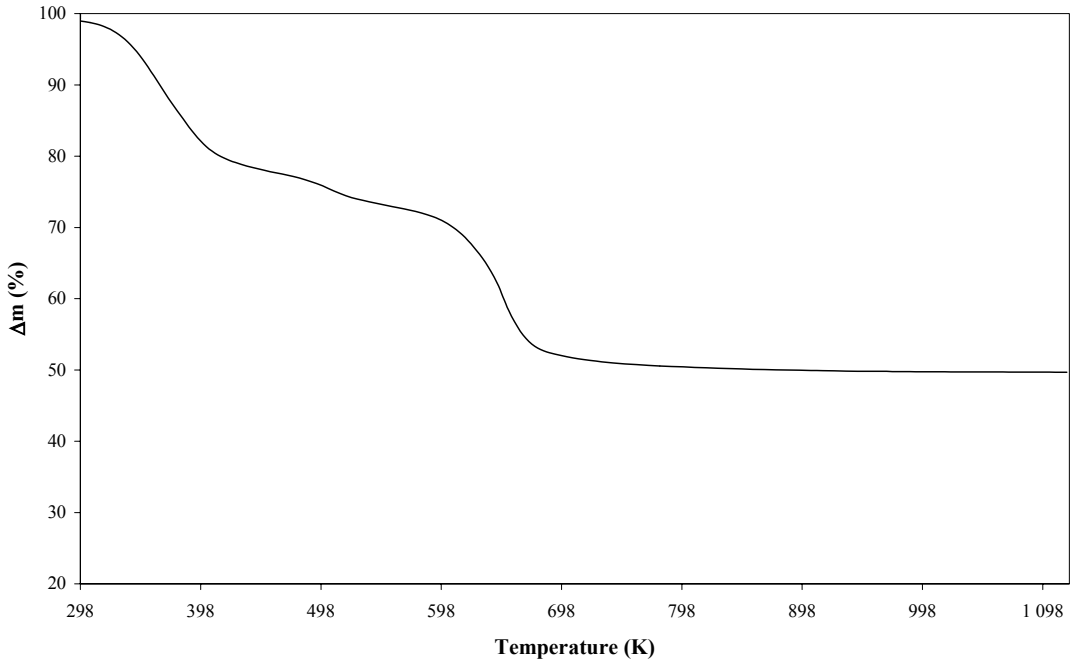

Fig.V.2: Thermogram of sol-gel precursor of $NiMoO_4$ dispersed on magnesia (Mg/Mo =5).

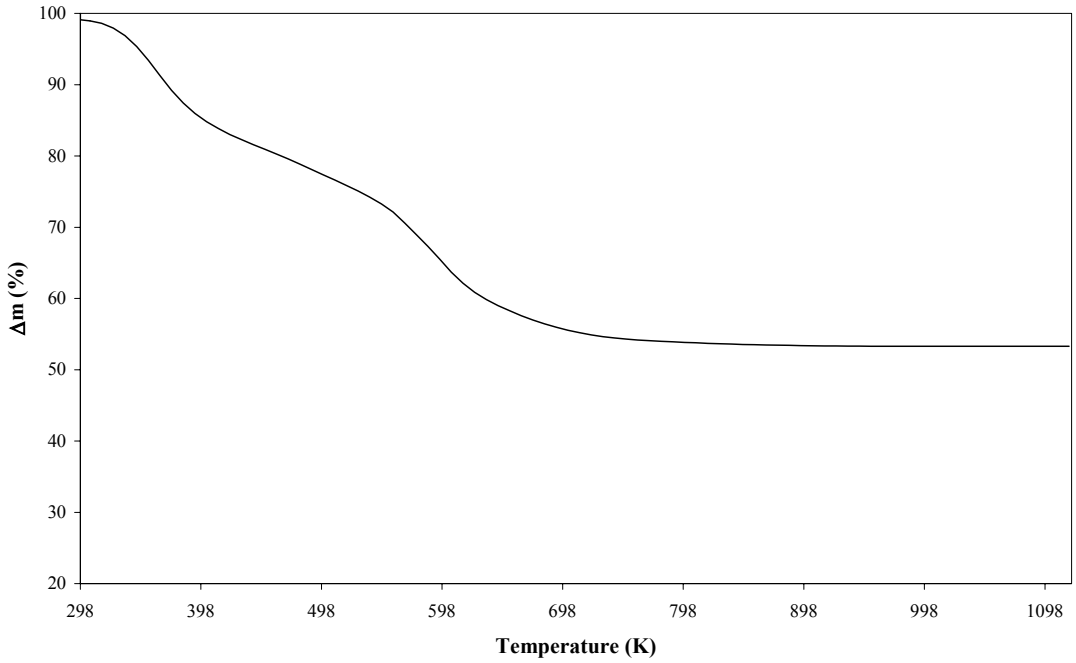

Fig.V.3: Thermogram of sol gel precursor of $NiMoO_4$ dispersed on alumina-magnesia ((Al+Mg)/Mo = 5).

V.1.3 X-ray diffraction and Raman spectroscopy

Table V.1: Composition and crystalline phases detected in all dispersed mixed Ni-Co molybdates prepared by sol-gel and impregnation methods.

Composition	Molar Ratio	Detected Crystalline Phases	
		Sol-gel	Impregnation
Ni :Mo :Al	1:1 :5	β-$NiMoO_4$	α and β-$NiMoO_4$
Ni :Co :Mo :Al	0.75:0.25:1:5	β-$Ni_{0.75}Co_{0.25}MoO_4$	β-$Ni_{0.75}Co_{0.25}MoO_4$
Ni :Co :Mo :Al	0.5:0.5:1:5	β-$Ni_{0.5}Co_{0.5}MoO_4$	β-$Ni_{0.5}Co_{0.5}MoO_4$
Ni :Co :Mo :Al	0.25:0.75:1:5	β-$Ni_{0.25}Co_{0.75}MoO_4$	β-$Ni_{0.25}Co_{0.75}MoO_4$
Co :Mo :Al	1:1 :5	β-$CoMoO_4$	β-$CoMoO_4$
Ni :Mo :Mg	1:1 :5	β-$NiMoO_4$ MgO	β-$NiMoO_4$ MgO
Ni :Co :Mo :Mg	0.75:0.25:1:5	β-$Ni_{0.75}Co_{0.25}MoO_4$ MgO	β-$Ni_{0.75}Co_{0.25}MoO_4$ MgO
Ni :Co :Mo :Mg	0.5:0.5:1:5	β-$Ni_{0.5}Co_{0.5}MoO_4$ MgO	β-$Ni_{0.5}Co_{0.5}MoO_4$ MgO
Ni :Co :Mo :Mg	0.25:0.75:1:5	β-$Ni_{0.25}Co_{0.75}MoO_4$ MgO	β-$Ni_{0.25}Co_{0.75}MoO_4$ MgO
Co :Mo :Mg	1:1 :5	β-$CoMoO_4$ MgO	β-$CoMoO_4$ MgO
Ni :Mo: (Al+Mg)	1:1 :5	β-$NiMoO_4$	-
Ni :Co :Mo :(Al+Mg)	0.75:0.25:1:5	Poorly resolved spectrum	-
Ni :Co :Mo:(Al+Mg)	0.5:0.5:1:5	Poorly resolved spectrum	-
Ni :Co :Mo : (Al+Mg)	0.25:0.75:1:5	β-$Ni_{0.25}Co_{0.75}MoO_4$	-
Co :Mo : (Al+Mg)	1:1 :5	$CoAl_2O_4$	-

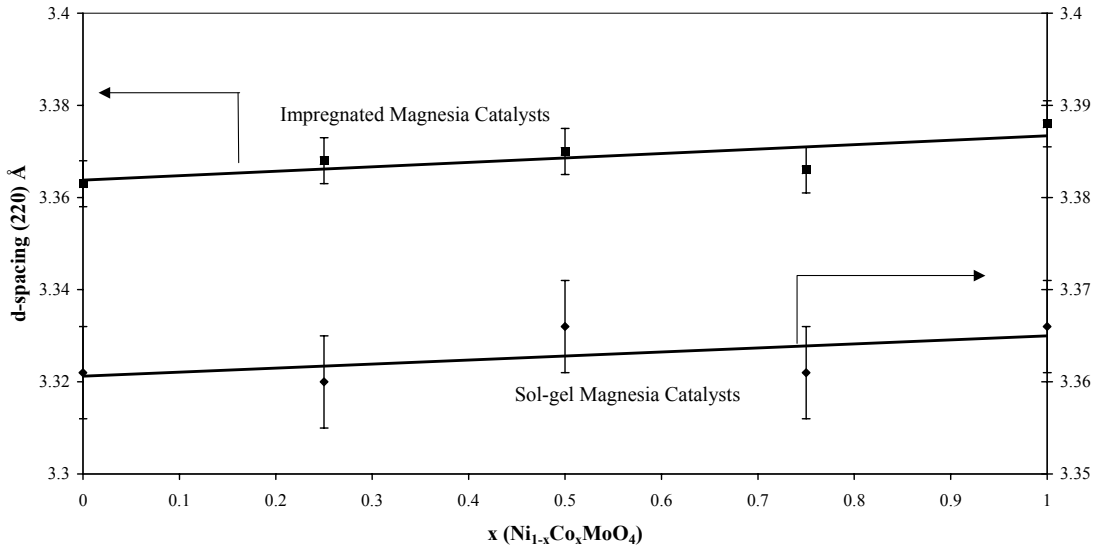

Fig.V.4: Verification of Vegard's law with the interreticular (220) d-spacing in $Ni_{1-x}Co_xMoO_4$ dispersed on magnesia (Mg/Mo = 5). (♦) β-$Ni_{1-x}Co_xMoO_4$ dispersed on MgO, prepared by the sol-gel method; (■) β-$Ni_{1-x}Co_xMoO_4$ supported on MgO, prepared by impregnation.

Table V.2: Raman data of some alumina- and magnesia-dispersed Ni-Co molybdates obtained by the sol-gel (S-g) and the impregnation (Imp).

Composition	Molar Ratio	Raman Shift (cm^{-1})
Ni :Mo :Al (S-g)	1:1 :5	959-946 (vs), 903-894 (s), 829 (m), 372 (m)
Ni :Co :Mo :Al (S-g)	0.75:0.25:1:5	954-945 (vs), 898 (m), 827 (m), 374(m), 343 (m)
Ni :Co :Mo :Al (S-g)	0.5:0.5:1:5	948-939 (vs), 880 (w), 818 (m), 421 (w), 369-351 (m), 333-329 (m)
Ni :Co :Mo :Al (S-g)	0.25:0.75:1:5	950-940 (vs), 878 (w), 818 (m), 421 (w), 368-352 (m), 339-327 (m)
Co :Mo :Al (S-g)	1:1 :5	949-938 (vs), 875 (m), 816 (s), 692 (w), 623 (w) 482 (w), 422 (w), 369-351 (m), 339-327 (m)
Ni :Mo :Al (Imp)	1:1 :5	962 (vs), 912 (s), 829 (w), 706 (m), 490 (w),416 (w), 387 (w), 367 (w)
Ni :Co :Mo :Al (Imp)	0.5:0.5:1:5	952-940 (vs), 887 (m), 818 (s), 426 (w), 375-366 (m), 342-333 (m)
Co :Mo :Al (Imp)	1:1 :5	948-938 (vs), 876 (m), 814 (s), 866 (m), 614 (w), 480 (w), 421 (w), 365 (m), 337-327 (m)
Ni :Mo :Mg (S-g)	1:1 :5	966-957 (vs), 908 (s), 849 (m), 533 (s), 380-369 (m), 349 –335 (m)
Ni :Co :Mo :Mg (S-g)	0.5:0.5:1:5	945* (vs), 891 (s), 827 (s), 648 (w), 456 (w), 365* (m), 341-332 (m)
Ni :Mo :Mg (Imp)	1:1 :5	970-957 (vs), 907 (s), 853 (w), 381-369 (s), 348-334 (s)
Ni :Co:Mo:Mg (Imp)	0.5:0.5:1:5	966-954 (vs), 910 (vs), 560 (w), 368 (m), 331 (m)
Co :Mo :Mg (Imp)	1:1 :5	954 (w), 680 (vs), 613 (w), 474 (s), 345 (w)

Table V.2 lists the main Raman shifts of all Al_2O_3- and MgO-dispersed catalysts. When comparing these data with those of the reference materials (169-171), we can conclude that the Raman spectra of all the alumina-dispersed Ni-Mo, Co-Mo and Ni-Co-Mo samples are in agreement with the XRD results. The only exception is

the Ni-Mo sample prepared by impregnation, in which Raman spectroscopy revealed only the α-phase of $NiMoO_4$.

The Raman spectra of the MgO-dispersed Ni-Mo, Co-Mo and Ni-Co-Mo samples are also in agreement with the XRD results: in all Ni-Co molybdates, the lines can be attributed to the β-phase.

V.1.4 Specific surface area and porosity measurements

Table V.3: Specific surface area measurements of all alumina-, magnesia- and Al_2O_3-MgO-dispersed $Ni_{1-x}Co_xMoO_4$.

Composition	Molar Ratio	S_{BET} (m^2 g^{-1})	
		Sol-gel	Impregnation
Ni :Mo :Al	1:1 :5	92	94
Ni :Co :Mo :Al	0.75:0.25:1:5	83	87
Ni :Co :Mo :Al	0.5:0.5:1:5	57	92
Ni :Co :Mo :Al	0.25:0.75:1:5	39	80
Co :Mo :Al	1:1 :5	38	88
Ni :Mo :Mg	1:1 :5	120	17
Ni :Co :Mo :Mg	0.75:0.25:1:5	125	18
Ni :Co :Mo :Mg	0.5:0.5:1:5	98	18
Ni :Co :Mo :Mg	0.25:0.75:1:5	78	28
Co :Mo :Mg	1:1 :5	100	24
Ni :Mo :(Al+Mg)	1:1 :5	80	-
Ni :Co :Mo :(Al+Mg)	0.75:0.25:1:5	50	-
Ni :Co :Mo:(Al+Mg)	0.5:0.5:1:5	86	-
Ni :Co :Mo : (Al+Mg)	0.25:0.75:1:5	59	-
Co :Mo : (Al+Mg)	1:1 :5	112	-

V.1.5 X-Ray photoelectron spectroscopy

Tables V.5-7 summarize the experimental atomic intensity ratios measured by XPS for all Al_2O_3-, MgO and Al_2O_3-MgO-dispersed catalysts; the values are compared with the theoretical ones (corresponding to the bulk composition).

Table V.4 lists the binding energy ranges of all elements present in alumina-, magnesia- and Al_2O_3-MgO dispersed catalysts.

TableV.4: XPS binding energies (eV) of all elements present in the catalysts.

Element	Al_2O_3	MgO	Al_2O_3-MgO
Ni $2p_{3/2}$	856.2 ± 0.1	855.3 ± 0.1	855.7 ± 0.1
Co $2p_{3/2}$	781.3 ± 0.2	780.3 ± 0.1	780.8 ± 0.2
Mo(VI) $3d_{5/2}$	232.8 ± 0.3	232.8 ± 0.2	232.5 ± 0.1
Mo(V) $3d_{5/2}$	231.8 ± 0.3	231.7 ± 0.2	-
Al 2p	74.4 ± 0.2	-	73.9 ± 0.1
Mg 2s	-	88.3 ± 0.2	88.8 ± 0.1

All the elements appear in their normally expected oxidation states: $Ni^{(II)}$, $Co^{(II)}$, $Mg^{(II)}$ and $Al^{(III)}$. The XPS spectra of molybdenum has been resolved into two components corresponding to Mo^{VI} and Mo^{V}, except in the case of Al_2O_3-MgO-dispersed catalysts, where this was not possible. The experimental (Mo^{VI}/Mo_{tot}) ratio of sol-gel catalysts is lower than in the impregnated catalysts.

It must be noticed that the binding energies of Ni $2p_{3/2}$ and Co $2p_{3/2}$ of Al_2O_3-MgO dispersed catalysts are intermediate between those measured in Al_2O_3 and MgO, suggesting a continuous variation in the interaction between the elements and the support.

Table V.5: Relative atomic intensity ratios measured by XPS in the alumina-supported Ni-Co molybdates prepared by the sol-gel and the impregnation method.

Composition	Ni/Mo		Co/Mo		Ni/Co		Ni/Al		Co/Al		Mo/Al	
	Exp.	Th.	Exp.	Th.	Exp.	Th.	Exp.	Th.	Exp.	Th.	Exp.	Th.
Ni :Mo :Al[i] (S-g)	0.4	1	-	-	-	-	0.38	0.2	-	-	0.38	0.2
Ni :Co :Mo :Al[ii] (S-g)	0.35	0.75	0.11	0.25	3	3	0.087	0.15	0.03	0.05	0.25	0.2
Ni :Co :Mo :Al[iii] (S-g)	0.24	0.5	0.22	0.5	1.08	1	0.06	0.1	0.055	0.1	0.25	0.2
Ni :Co :Mo :Al[iv] (S-g)	0.16	0.25	0.35	0.75	0.45	0.33	0.036	0.05	0.08	0.15	0.22	0.2
Co :Mo :Al[i] (S-g)	-	-	0.42	1	-	-	-	-	0.14	0.2	0.33	0.2
Ni :Mo :Al[i] (Imp)	0.63	1	-	-	-	-	0.46	0.2	-	-	0.73	0.2
Ni :Co :Mo :Al[ii] (Imp)	0.48	0.75	0.19	0.25	2.53	3	0.51	0.15	0.20	0.05	1.06	0.2
Ni :Co :Mo :Al[iii] (Imp)	0.28	0.5	0.29	0.5	0.85	1	0.29	0.1	0.34	0.1	1.01	0.2
Ni :Co :Mo :Al[iv] (Imp)	0.17	0.25	0.57	0.75	0.29	0.33	0.33	0.05	1.15	0.15	2.0	0.2
Co :Mo :Al[i] (Imp)	-	-	0.59	1	-	-	-	-	1.05	0.2	1.77	0.2

Molar Ratios: (i) = 1:1:5; (ii) = 0.75:0.25:1:5; (iii) = 0.5:0.5:1:5 (iv) = 0.25:0.75:1:5

Table V.6: Relative atomic intensity ratios measured by XPS in the magnesia-supported Ni-Co molybdates prepared by the sol-gel and the impregnation method.

Composition	Ni/Mo		Co/Mo		Ni/Co		Ni/Mg		Co/Mg		Mo/Mg	
	Exp.	Th.	Exp.	Th.	Exp.	Th.	Exp.	Th.	Exp.	Th.	Exp.	Th.
Ni :Mo :Mg[i] (S-g)	0.62	1	-	-	-	-	0.09	0.2	-	-	0.15	0.2
Ni :Co :Mo :Mg[ii] (S-g)	0.57	0.75	0.26	0.25	2.23	3	0.10	0.15	0.045	0.05	0.18	0.2
Ni :Co :Mo :Mg[iii] (S-g)	0.5	0.5	0.61	0.5	0.83	1	0.08	0.1	0.09	0.1	0.15	0.2
Ni :Co :Mo :Mg[iv] (S-g)	0.29	0.25	0.61	0.75	0.48	0.33	0.047	0.05	0.10	0.15	0.16	0.2
Co :Mo :Mg[i] (S-g)	-	-	0.85	1	-	-	-	-	0.12	0.2	0.15	0.2
Ni :Mo :Mg[i] (Imp)	0.67	1	-	-	-	-	0.34	0.2	-	-	0.51	0.2
Ni :Co :Mo :Mg[ii] (Imp)	0.57	0.75	0.17	0.25	3.2	3	0.41	0.15	0.13	0.05	0.72	0.2
Ni :Co:Mo :Mg[iii] (Imp)	0.45	0.5	0.25	0.5	1.83	1	0.31	0.1	0.17	0.1	0.68	0.2
Ni :Co:Mo :Mg[iv] (Imp)	0.32	0.25	0.42	0.75	0.76	0.33	0.13	0.05	0.17	0.15	0.4	0.2
Co :Mo :Mg[i] (Imp)	-	-	0.66	1	-	-	-	-	0.26	0.2	0.4	0.2

Molar Ratios: (i) = 1:1:5; (ii) = 0.75:0.25:1:5; (iii) = 0.5:0.5:1:5 (iv) = 0.25:0.75:1:5

Table V.7: Relative atomic intensity ratios measured by XPS in the Al_2O_3-MgO-supported Ni-Co molybdates prepared by the sol-gel method.

Composition	Ni/Mo		Co/Mo		Ni/Co		Ni/(Al+Mg)		Co/(Al+Mg)		Mo/(Al+Mg)	
	Exp.	Th.	Exp.	Th.	Exp.	Th.	Exp.	Th.	Exp.	Th.	Exp.	Th.
Ni :Mo :(Al+Mg)[i]	0.58	1	-	-	-	-	0.079	0.2	-	-	0.136	0.2
Ni :Co :Mo :(Al+Mg)[ii]	0.49	0.75	0.33	0.25	1.51	3	0.066	0.15	0.04	0.05	0.134	0.2
Ni :Co :Mo :(Al+Mg)[iii]	0.53	0.5	0.56	0.5	0.94	1	0.075	0.1	0.08	0.1	0.142	0.2
Ni :Co :Mo :(Al+Mg)[iv]	0.18	0.25	0.42	0.75	0.43	0.33	0.028	0.05	0.06	0.15	0.153	0.2
Co :Mo :(Al+Mg)[i]	-	-	0.79	1	-	-	-	-	0.12	0.2	0.154	0.2

Molar Ratios: (i) = 1:1:5; (ii) = 0.75:0.25:1:5; (iii) = 0.5:0.5:1:5 (iv) = 0.25:0.75:1:5

V.2 Titania- and zirconia-supported catalysts prepared by impregnation

V.2.1 Characterization of the pure supports

Commercial titania and zirconia samples used in the present work correspond to anatase (tetragonal) (file 21-1272) and baddeleyite (monoclinic) (file 37-1484), respectively. In Raman spectroscopy, anatase was easily identified by means of the lines at 704, 673, 511, 394, 197, 186, 167 and 143 cm^{-1}, while baddeleyite displayed lines at 636-613, 558-536, 501-474, 383, 346-332, 306, 223, 203 and 189-178 cm^{-1}.

The isotherms of both commercial titania and zirconia exhibit a shape corresponding to type II in Brunauer's classification.

The specific surface area of TiO_2 was found to be equal to 8 $m^2 g^{-1}$; this support is characterized by a Vp equal to 0.07 $cm^3 g^{-1}$ and a Dp of 49.5 nm.

The specific surface area of commercial ZrO_2 was equal to 6 $m^2 g^{-1}$; this support is characterized by a Vp equal to 0.04 $cm^3 g^{-1}$ and a Dp of 19.5 nm.

V.2.2 X-ray diffraction, Raman spectroscopy and S_{BET} measurements

Table V.8 lists all TiO_2- and ZrO_2-supported catalysts prepared by impregnation with their respective BET specific surface areas and the crystalline phases identified by X-ray diffraction.

Table V.9 lists the Raman shifts of the most intense lines in all titania- and zirconia-supported $Ni_{1-x}Co_xMoO_4$. When comparing with the reference data (102-104), we can conclude that the Raman spectra of all the Ni-Mo, Co-Mo and Ni-Co-Mo samples are generally in agreement with the XRD results. In TiO_2-supported Ni-Mo besides the β-phase, the distorted α'- $NiMoO_4$ phase is also detected.

Table V.8: Composition, specific surface area and crystalline phases detected in TiO_2- and ZrO_2-supported mixed Ni-Co molybdates.

Composition	Molar Ratio	Detected Crystalline Phases	S_{BET} ($m^2 g^{-1}$)
Ni :Mo :Ti	1:1 :5	β-$NiMoO_4$, TiO_2	14
Ni :Co :Mo :Ti	0.75:0.25:1:5	β-$Ni_{0.75}Co_{0.25}MoO_4$, TiO_2	12
Ni :Co :Mo: Ti	0.5:0.5:1:5	β-$Ni_{0.5}Co_{0.5}MoO_4$, TiO_2	12
Ni :Co :Mo : Ti	0.25:0.75:1:5	β-$Ni_{0.25}Co_{0.75}MoO_4$, TiO_2	9
Co :Mo : Ti	1:1 :5	$CoMoO_4$, TiO_2	6
Ni :Mo :Zr	1:1 :5	α-$NiMoO_4$, ZrO_2	12
Ni :Co :Mo :Zr	0.75:0.25:1:5	β-$Ni_{0.75}Co_{0.25}MoO_4$, ZrO_2	9
Ni :Co :Mo: Zr	0.5:0.5:1:5	β-$Ni_{0.5}Co_{0.5}MoO_4$, ZrO_2	8
Ni :Co :Mo : Zr	0.25:0.75:1:5	β-$Ni_{0.25}Co_{0.75}MoO_4$, ZrO_2	9
Co :Mo : Zr	1:1 :5	$CoMoO_4$, ZrO_2	8

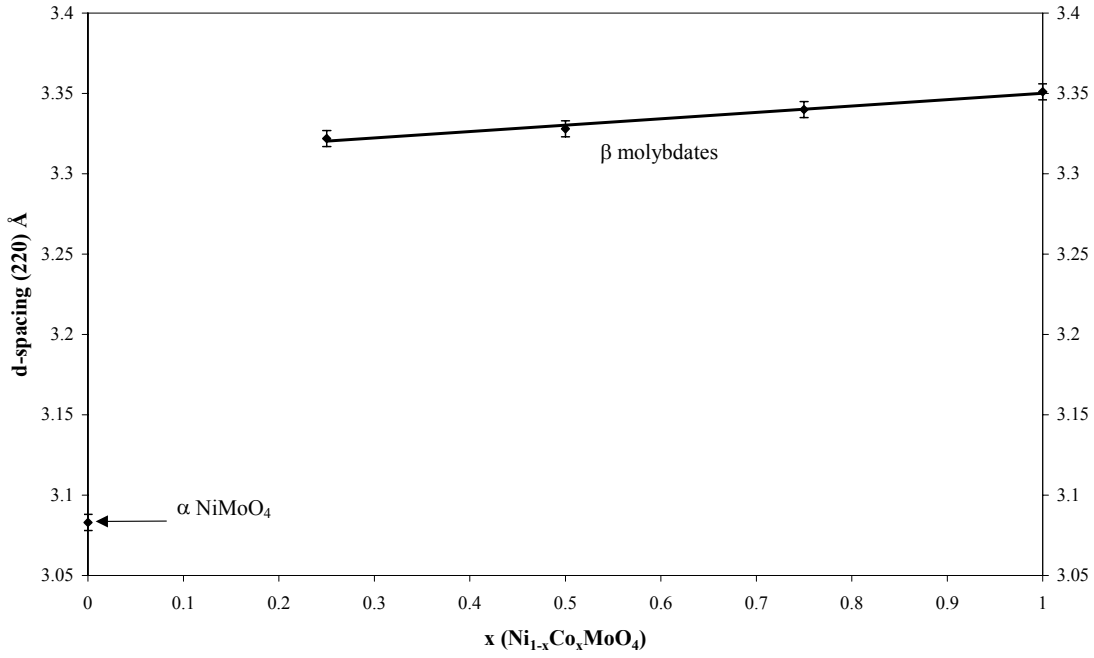

Fig.V.5: Verification of Vegard's law with the interreticular (220) d-spacing in $Ni_{1-x}Co_xMoO_4$ supported on zirconia (Zr/Mo = 5), prepared by impregnation

Table V.9: Raman data of titania- and zirconia supported Ni-Co molybdates.

Composition	Molar Ratio	Raman Shift (cm^{-1})
Ni :Mo :Ti	1:1 :5	956-944 (s), 908-897 (w), 827 (m), 633 (vs), 508 (vs), 394 (m), 199 (s); 961 (vs), 911 (s), 829 (w), 705 (m), 634 (vs), 511 (vs), 393 (vs), 198 (m)
Ni :Co :Mo :Ti	0.75:0.25:1:5	954* (s), 904 (w), 820 (w), 702 (w), 635(vs), 510 (vs) 395 (vs), 198 (s)
Ni :Co :Mo :Ti	0.5:0.5:1:5	939* (s), 885 (w), 810 (w), 629 (vs), 506 (vs), 390 (vs), 198 (vs)
Ni :Co :Mo :Ti	0.25:0.75:1:5	932* (s), 879 (w), 813 (w), 627 (vs), 506 (vs), 391 (vs), 199 (s)
Co :Mo :Ti	1:1 :5	930* (s), 872 (m), 809 (m), 629 (vs), 507 (vs), 390 (vs), 199 (s)
Ni :Mo :Zr	1:1 :5	961 (vs), 911 (s), 704 (s), 635-613 (s), 556-532 (m), 502-473 (s), 413 (w), 376 (s), 342-331 (s), 301 (w), 219 (m), 186-178 (s)
Ni :Co :Mo :Zr	0.75:0.25:1:5	952-940 (vs), 903 (m), 820 (w), 702 (m), 635-613 (s), 554-531 (m), 498-470 (vs), 375 (s), 343-330 (vs), 299 (s), 219 (s), 204 (w), 186-178 (s)
Ni :Co :Mo :Zr	0.5:0.5:1:5	952-939 (vs), 886 (m), 819 (m), 702 (w), 632-611 (vs), 499-473 (vs), 376(vs), 344-331 (vs), 301 (m), 218 (s), 188-178 (vs)
Ni :Co :Mo :Zr	0.25:0.75:1:5	947-937 (vs), 880 (s), 814 (s), 633-611 (s), 553-531 (w), 499-473 (s), 375 (s), 341-331 (s), 299 (w), 219 (w), 188-178 (m)
Co :Mo :Zr	1:1 :5	945-935 (vs), 880 (w), 817 (s), 633-610 (vs), 556-531 (m), 498-472 (vs), 376 (vs), 331* (vs), 299 (m), 219 (m), 187-177 (s)

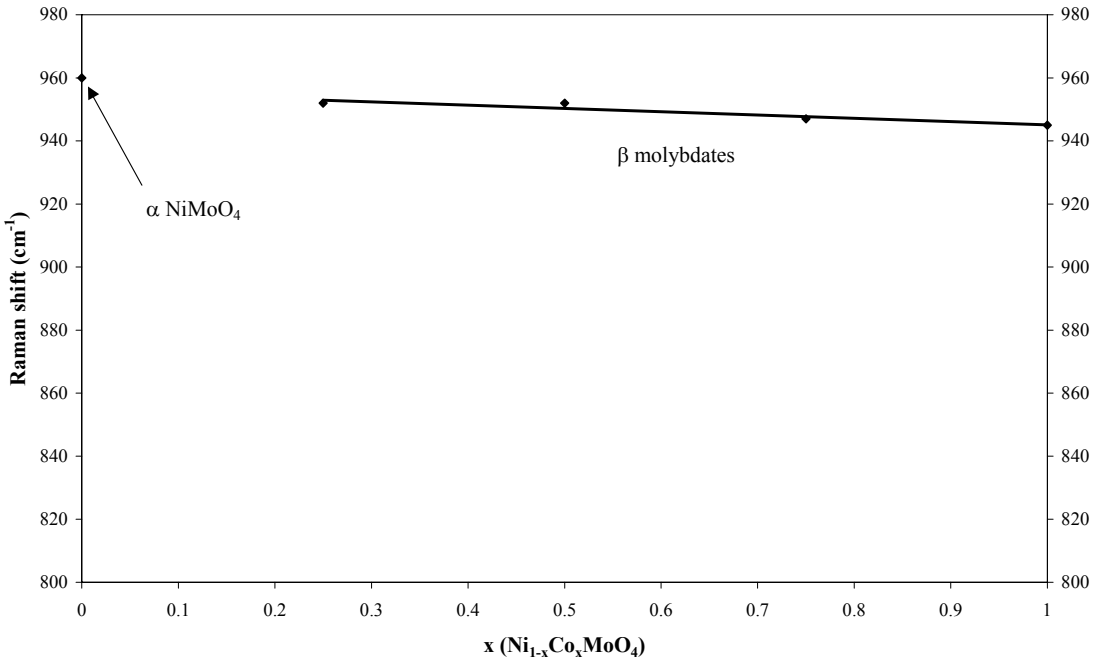

Fig.V.6: Evolution of the Raman shift of the $NiMoO_4$ line at 960 cm^{-1} with respect to the Ni/Co composition in ZrO_2-supported $Ni_{1-x}Co_xMoO_4$.

V.2.3 X-ray photoelectron spectroscopy

Table V.10 summarizes the experimental atomic intensity ratios measured by XPS for all TiO_2- and ZrO_2-supported samples; the values are compared with the theoretical ones (corresponding to the bulk composition).

Table V.10: Relative atomic intensity ratios measured by XPS in the titania- and zirconia-supported Ni-Co molybdates, prepared by impregnation.

Composition	Ni/Mo		Co/Mo		Ni/Co		Ni/Supp		Co/Supp		Mo/Supp	
	Exp.	Th.	Exp.	Th.	Exp.	Th.	Exp	Th.	Exp.	Th.	Exp.	Th.
Ni :Mo :Ti[i]	0.67	1	-	-	-	-	1.43	0.2	-	-	2.15	0.2
Ni :Co :Mo :Ti[ii]	0.52	0.75	0.21	0.25	2.39	3	0.84	0.15	0.35	0.05	1.68	0.2
Ni :Co :Mo :Ti[iii]	0.31	0.5	0.33	0.5	0.98	1	0.58	0.1	0.6	0.1	1.83	0.2
Ni :Co :Mo :Ti[iv]	0.2	0.25	0.45	0.75	0.45	0.33	0.28	0.05	0.62	0.15	1.38	0.2
Co :Mo :Ti[i]	-	-	0.52	1	-	-	-	-	0.5	0.2	0.96	0.2
Ni :Mo :Zr[i]	0.7	1	-	-	-	-	4.03	0.2	-	-	5.77	0.2
Ni :Co :Mo :Zr[ii]	0.53	0.75	0.24	0.25	2.17	3	4.86	0.15	2.23	0.05	9.15	0.2
Ni :Co :Mo :Zr[iii]	0.33	0.5	0.33	0.5	1	1	1.58	0.1	1.58	0.1	4.86	0.2
Ni :Co :Mo :Zr[iv]	0.18	0.25	0.53	0.75	0.34	0.33	0.98	0.05	2.92	0.15	5.46	0.2
Co :Mo :Zr[i]	-	-	0.69	1	-	-	-	-	3.16	0.2	4.56	0.2

All the elements present in table V.11 appear in their normally expected oxidation states: $Ni^{(II)}$, $Co^{(II)}$, $Ti^{(IV)}$ and $Zr^{(IV)}$. The XPS spectra of molybdenum were again resolved into two components corresponding to Mo^{VI} and Mo^{V}, the ratio between these two species being approximately the same in both type of catalysts.

TableV.11: XPS binding energies (eV) of all elements present in the catalysts.

Element	TiO_2	ZrO_2
Ni $2p_{3/2}$	855.9 ± 0.1	856.1 ± 0.1
Co $2p_{3/2}$	781.1 ± 0.2	781.2 ± 0.1
Mo(VI) $3d_{5/2}$	232.7 ± 0.2	232.7 ± 0.1
Mo(V) $3d_{5/2}$	231.7 ± 0.2	231.7 ± 0.2
Ti $2p_{3/2}$	458.7 ± 0.2	-
Zr $3d_{5/2}$	-	182.3 ± 0.1

V.3 Catalytic performances

V.3.1 Catalytic behavior of alumina-supported Ni and Co molybdates

Tables V.12 and 13 list the catalytic performances of the alumina-supported catalysts prepared by sol-gel and impregnation method, respectively. For comparison, pure alumina prepared by the sol-gel method shows a good catalytic activity at 753 K, displaying a $XC_3°$ of 8.7 %; however, the main product is CO_2 ($YCO_2/3$ = 4.1 %), even if a certain amount of propene is produced ($YC_3^=$ = 1.9 %). In the case of the sol-gel prepared catalysts, the incorporation of the active phase on alumina leads to an enhancement of the values of $XC_3°$ and $YC_3^=$. Mixed Ni-Co molybdates show lower XO_2 and $YCO_2/3$ than alumina, on one hand, while simple Ni and Co molybdates show higher XO_2 and $YCO_2/3$ than alumina, on the other hand. The situation is very different in the case of impregnated alumina-catalysts. Generally speaking, the incorporation of the active phase on commercial alumina leads to a decrease of $XC_3°$, $YC_3^=$, XO_2 and $YCO_2/3$. In the next section the most illustrative results and trends will be listed and commented.

V.3.2 Catalytic behavior of magnesia-supported Ni and Co molybdates

Tables V.14 and V.15 show the catalytic performances of magnesia-dispersed catalysts prepared by the sol-gel method and impregnation method, respectively. For comparison, magnesia prepared by sol-gel method shows a very low catalytic activity at 753 K ($XC_3°$ = 2.8 %), and produces mainly CO_2, even if a certain amount of propene is detected. In the case of the sol-gel prepared catalysts, the incorporation of the active phase on magnesia leads to an enhancement of the values of $XC_3°$, $YC_3^=$. Oxygen conversion and CO_2 yield values remain almost unchanged. The situation is very different in the case of impregnated magnesia-catalysts. Generally speaking, the incorporation of the active phase on commercial magnesia leads to an increase of $XC_3°$, $YC_3^=$, XO_2 and $YCO_2/3$ values.

Table V.12: Catalytic results in propane ODH for alumina-dispersed Ni-Co-molybdates prepared by sol-gel method.

Composition	Temperature (K)	$XC_3°$ (%)	$YC_3^=$ (%)	$SC_3^=$ (%)	XO_2 (%)	$YCO_2/3$ (%)	SCO_2 (%)	C Balance
Al_2O_3	723	5.0	1.3	25.0	17.5	2.4	48.3	73 %
	753	8.7	1.9	21.3	30.5	4.1	46.6	68 %
Ni:Mo:Al	723	11.7	1.9	16.5	39.8	7.4	63.0	79 %
1:1:5	753	15.9	3.3	21.0	47.6	8.2	51.7	73 %
Ni:Co:Mo:Al	723	6.2	2.5	40.9	11.4	1.8	29.5	70 %
0.75: 0.25:1:5	753	10.6	4.0	38.1	21.6	3.4	32.1	70 %
Ni:Co:Mo:Al	723	8.8	4.1	46.4	18.1	3.1	35.1	82 %
0.5: 0.5:1:5	753	12.8	5.0	39.2	27.8	4.4	34.5	74 %
Ni:Co:Mo:Al	723	7.3	4.5	62.1	14.8	2.1	29.1	91 %
0.25: 0.75:1:5	753	11.1	5.0	45.2	20.6	3.1	27.8	73 %
Co:Mo:Al	723	20.5	8.8	42.9	58.8	9.6	47.0	90 %
1:1:5	753	25.4	9.6	37.8	73.1	11.6	45.7	84 %

Table V.13: Catalytic results in propane ODH for alumina-supported Ni-Co-molybdates prepared by impregnation method.

Composition	Temperature (K)	$XC_3°$ (%)	$YC_3^=$ (%)	$SC_3^=$ (%)	XO_2 (%)	$YCO_2/3$ (%)	SCO_2 (%)	C Balance
Ni:Mo:Al	723	5.6	3.8	67.7	11.9	1.5	27.5	95 %
1:1:5	753	11.3	5.5	48.9	25.0	3.1	27.4	76 %
Ni:Co:Mo:Al	723	8.7	1.5	17.3	27.3	5.8	66.2	84 %
0.75: 0.25:1:5	753	14.9	4.0	27.0	42.3	8.8	59.3	86 %
Ni:Co:Mo:Al	723	4.9	3.1	62.6	11.4	1.5	31.6	94 %
0.5: 0.5:1:5	753	10.2	5.5	53.9	24.5	3.1	30.4	84 %
Ni:Co:Mo:Al	723	6.4	2.7	42.1	10.2	1.3	20.4	63 %
0.25: 0.75:1:5	753	9.9	4.8	48.5	17.7	2.3	23.5	72 %
Co:Mo:Al	723	5.1	3.7	72.3	8.6	0.7	14.5	87 %
1:1:5	753	11.6	5.3	45.7	18.5	*1.5*	*13.0*	59 %

Table V.14: Catalytic results in propane ODH for magnesia-dispersed Ni-Co-molybdates prepared by sol-gel method.

Composition	Temperature (K)	$XC_3°$ (%)	$YC_3^=$ (%)	$SC_3^=$ (%)	XO_2 (%)	$YCO_2/3$ (%)	SCO_2 (%)	C Balance
MgO	753	*2.8*	*0.7*	*26.7*	*15.6*	*3.3*	*118.2*	*> 100 %*
Ni:Mo:Mg	723	*5.0*	*0.5*	*10.9*	*11.3*	*2.1*	*41.7*	*53 %*
1:1:5	753	*8.8*	*1.3*	*14.8*	*14.9*	*2.7*	*31.1*	*46 %*
Ni:Co:Mo:Mg	723	1.9	-	-	9.8	-	-	-
0.75: 0.25:1:5	753	2.5	-	-	13.1	-	-	-
Ni:Co:Mo:Mg	723	5.4	2.7	49.4	8.0	1.0	18.4	68 %
0.5: 0.5:1:5	753	11.3	4.5	39.5	10.4	1.4	12.8	52 %
Ni:Co:Mo:Mg	723	8.4	4.1	49.3	25.5	5.3	63.4	> 100 %
0.25: 0.75:1:5	753	13.8	5.8	42.0	37.1	7.9	57.3	99 %
Co:Mo:Mg	723	3.4	1.3	39.1	-	0.7	20.8	60 %
1:1:5	753	6.9	4.1	60.1	14.6	2.5	36.0	96 %

Table V.15: Catalytic results in propane ODH for magnesia-supported Ni-Co-molybdates prepared by impregnation.

Composition	Temperature (K)	$XC_3°$ (%)	$YC_3^=$ (%)	$SC_3^=$ (%)	XO_2 (%)	$YCO_2/3$ (%)	SCO_2 (%)	C Balance
Ni:Mo:Mg	673	0.3	-	-	-	-	-	-
1:1:5	723	0.3	-	-	-	-	-	-
	753	1.3	-	-	-	-	-	-
Ni:Co:Mo:Mg	673	4.3	2.4	55.2	7.7	0.9	20.3	75 %
0.75: 0.25:1:5	723	6.6	3.9	58.7	14.2	2,0	31.0	90 %
	753	7.2	4.7	65.8	16.9	2.3	32.0	98 %
Ni:Co:Mo:Mg	673	2.2	1.5	65.9	5.7	0.8	36.9	≈ 100 %
0.5: 0.5:1:5	723	5.4	3.1	57.3	14.8	2.6	48.5	≈ 100 %
	753	7.9	4.6	58.1	20.8	3.8	47.4	≈ 100 %
Ni:Co:Mo:Mg	673	3.6	1.5	41.0	6.6	1.4	38.0	79 %
0.25: 0.75:1:5	723	7.3	3.8	51.5	17.8	3.5	47.3	99 %
	753	13.3	6.5	48.7	36.2	7.3	54.7	≈ 100 %
Co:Mo:Mg	673	1.8	0.7	40.0	8.0	1.0	55.9	96 %
1:1:5	723	6.9	1.4	20.1	26.2	5.2	75.6	96 %
	753	16.7	6.1	36.5	52.2	10.7	64.1	100 %

V.3.3 Catalytic behavior of Al_2O_3-MgO-supported Ni and Co molybdates

Table V.16 shows the catalytic performances of Al_2O_3-MgO-supported catalysts. For comparison, Al_2O_3-MgO support prepared by sol-gel method appears to be very active ($XC_3°$ = 12 %, at 753 K), even if the main observed product is CO_2. The incorporation of the active phase on alumina-magnesia support leads to an enhancement of the values $YC_3^=$; however, the values of $XC_3°$, XO_2 and $YCO_2/3$ are lower or close to those of pure alumina-magnesia support.

Table V.16: Catalytic results in propane ODH for Al_2O_3-MgO-supported Ni-Co-molybdates prepared by sol-gel method.

Composition	Temp. (K)	$XC_3°$ (%)	$YC_3^=$ (%)	$SC_3^=$ (%)	XO_2 (%)	$YCO_2/3$ (%)	SCO_2 (%)	C Balance
Al_2O_3-MgO	723	*8.6*	*0.0*	*0.0*	*25.3*	*4.6*	*53.3*	*53 %*
	753	*12.0*	*0.4*	*3.4*	*37.4*	*5.8*	*48.3*	*52 %*
Ni:Mo:(Al+Mg) 1:1:5	723	1.9	0.9	49.1	4.5	0.7	35.7	85 %
	753	3.3	1.3	40.6	8.5	1.1	32.1	73 %
Ni:Co:Mo: (Al+Mg) 0.75: 0.25:1:5	723	2.9	1.3	44.0	2.8	0.6	21.7	66 %
	753	5.1	2.3	45.1	3.8	1.1	22.1	67 %
Ni:Co:Mo: (Al+Mg) 0.5: 0.5:1:5	723	6.0	3.1	51.8	9.4	1.8	29.2	81 %
	753	10.2	4.7	45.7	20.8	3.3	31.8	77 %
Ni:Co:Mo: (Al+Mg) 0.25: 0.75:1:5	723	6.7	2.7	40.8	10.4	2.1	32.0	73 %
	753	11.2	4.7	42.3	16.7	2.9	26.1	68 %
Co:Mo: (Al+Mg) 1:1:5	753	22.2	8.1	36.5	65.1	12.3	55.3	92 %

V.3.4 Catalytic behavior of TiO_2-supported Ni and Co molybdates

Table V.17 shows the catalytic performances of TiO_2-supported catalysts. Commercial TiO_2 was tested in propane ODH, displaying a very low catalytic activity ($XC_3°$ = 1.6 % at 753 K). The incorporation of the active phase on commercial titania leads to an enhancement of the values of $XC_3°$, $YC_3^=$. Oxygen conversion and CO_2 yield values are lower than those displayed by titania, except for $Ni_{0.25}Co_{0.75}MoO_4$.

Figure V.7 shows the intrinsic propene yield ($Y*C_3^=$) of all TiO_2-supported Ni and Co molybdates. Taking into account the specific surface areas of these samples, it comes out that they all show good catalytic performances, which are close or higher than those of MgO-supported catalysts prepared by impregnation. The intrinsic propene yields vary between 0.7 % m^{-2} in $Ni_{0.5}Co_{0.5}MoO_4$ and 1.6 % m^{-2} in $Ni_{0.25}Co_{0.75}MoO_4$.

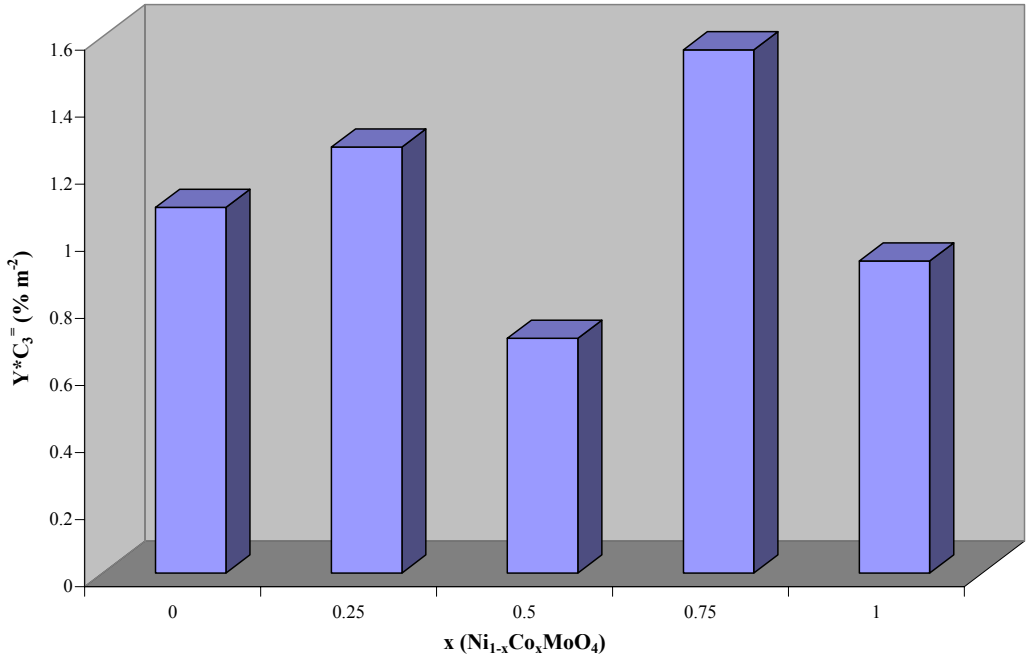

Fig.V.7: Evolution of the intrinsic propene yield ($Y^*C_3^=$) of TiO_2-supported catalysts with respect to the Co content (at 753 K).

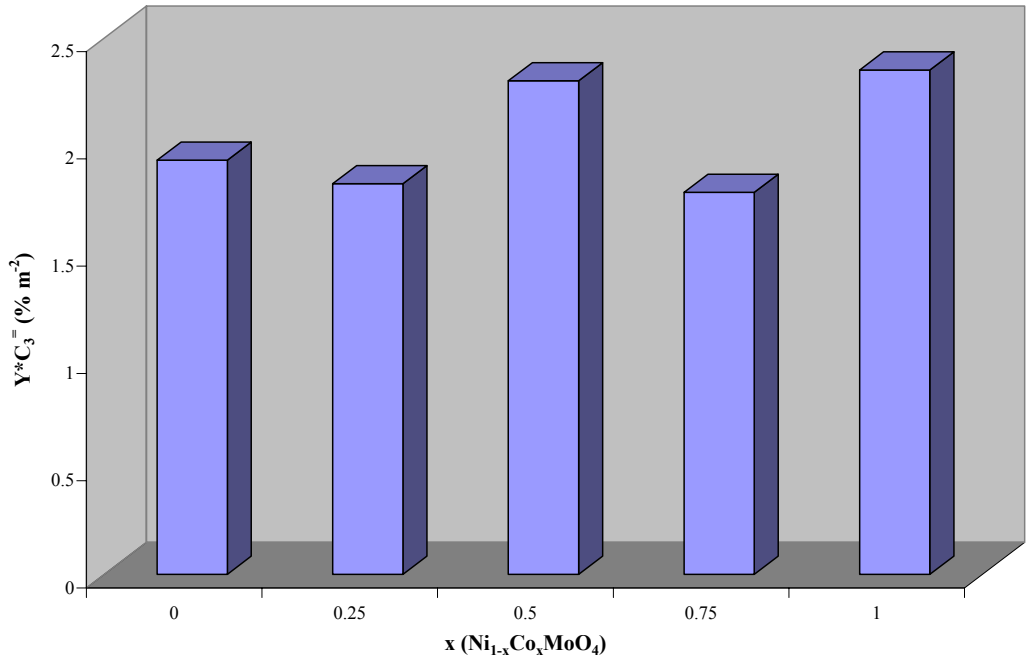

Fig.V.8: Evolution of the intrinsic propene yield ($Y^*C_3^=$) of ZrO_2-supported catalysts with respect to the Co content (at 753 K).

V.3.5 Catalytic behavior of ZrO_2-supported Ni and Co molybdates

Table V.18 shows the catalytic performances of ZrO_2-supported catalysts. Commercial ZrO_2 displays a good catalytic activity already at 723 K ($XC_3° = 6.6$ %) and both propene and CO_2 yields are characterized by the same value. When the active phase is incorporated in zirconia, an enhancement of the values of $YC_3^=$ is observed, propane conversion lowers or remains almost unchanged. In the Ni-rich catalysts (x = 0, 0.25), the oxygen conversion and the CO_2 yield are both improved.

Fig. V.8 shows the intrinsic propene yield ($Y^*C_3^=$) of all ZrO_2-supported Ni-Co-Mo prepared by impregnation. If we take into account the low specific surface areas of all these samples, they all display high propene intrinsic yields, going from 1.78 % m^{-2} in $Ni_{0.25}Co_{0.75}MoO_4$ to 2.35 % m^{-2} in $CoMoO_4$. Among the three mixed Ni-Co molybdates, $Ni_{0.5}Co_{0.5}MoO_4$ is the one showing the highest value of intrinsic propene yield.

Table V.17: Catalytic results in propane ODH for TiO_2-supported Ni-Co-molybdates prepared by impregnation.

Composition	Temperature (K)	$XC_3°$ (%)	$YC_3^=$ (%)	$SC_3^=$ (%)	XO_2 (%)	$YCO_2/3$ (%)	SCO_2 (%)	C Balance
TiO_2	723	1.5	0.0	0.0	3.2	0.4	24.7	25 %
	753	1.6	0.2	11.7	3.6	0.4	28.2	40 %
Ni:Mo:Ti	723	2.9	1.9	64.2	1.8	0.3	9.4	74 %
1:1:5	753	3.8	3.3	86.0	2.9	0.4	10.5	96 %
Ni:Co:Mo:Ti	723	4.4	0.0	0.0	14.6	3.6	81.7	82 %
0.75: 0.25:1:5	753	3.8	1.4	35.7	6.4	1.3	33.3	69 %
Ni:Co:Mo:Ti	723	1.3	1.0	71.4	0.3	0.2	17.9	89 %
0.5: 0.5:1:5	753	2.0	1.9	94.6	1.5	0.3	15.7	> 100 %
Ni:Co:Mo:Ti 0.25: 0.75:1:5	753	3.5	2.3	66.7	4.1	0.3	9.7	76 %
Co:Mo:Ti	723	0.8	0.7	80.0	0.6	0.2	23.3	≈ 100 %
1:1:5	753	1.4	1.2	80.2	2.1	0.2	16.2	96 %

Table V.18: Catalytic results in propane ODH for ZrO_2-supported Ni-Co-molybdates prepared by impregnation.

Composition	Temperature (K)	$XC_3°$ (%)	$YC_3^=$ (%)	$SC_3^=$ (%)	XO_2 (%)	$YCO_2/3$ (%)	SCO_2 (%)	C Balance
ZrO_2	723	6.6	0.9	13.9	11.4	1.0	15.5	29 %
	753	9.6	1.7	17.9	13.2	1.7	17.6	35 %
Ni:Mo:Zr	723	7.5	4.0	53.0	17.2	2.5	33.3	86 %
1:1:5	753	11.9	5.8	48.9	27.6	3.7	31.4	80 %
Ni:Co:Mo:Zr	723	7.4	2.7	36.0	20.0	2.7	36.7	73 %
0.75: 0.25:1:5	753	10.4	4.1	39.1	25.6	2.9	27.8	67 %
Ni:Co:Mo:Zr	723	3.5	2.7	76.8	5.7	0.5	13.6	90 %
0.5: 0.5:1:5	753	6.3	4.6	73.6	9.3	0.8	12.5	86 %
Ni:Co:Mo:Zr	723	3.2	2.4	73.7	4.4	0.5	16.7	90 %
0.25: 0.75:1:5	753	5.4	4.0	73.6	8.2	0.9	15.8	89 %
Co:Mo:Zr	723	2.6	1.9	73.8	3.6	0.4	14.8	87 %
1:1:5	753	4.7	3.4	72.1	6.0	0.6	13.6	86 %

V.4 Evaluation of the catalytic performances of Ni:Co:Mo:Supp with respect to the amount of Mg included in the formulation

Figs.V.9-10 display the catalytic performances of Ni:Co:Mo:Supp. (1-x:x:1:5, Supp. = Al_2O_3, Al_2O_3-MgO, MgO) prepared by the sol-gel method, expressed in terms of propane conversion ($XC_3°$) and absolute propene yield ($YC_3^=$) with respect to the amount of Mg included in the support. Generally speaking, in the case of $NiMoO_4$ and $CoMoO_4$ the higher the amount of Mg in the support, the lower the catalytic activity: however, it is worth remembering that these parameters are strongly affected by the specific surface areas of the samples.

The mixed Ni-Co molybdates behave somewhat differently: while $Ni_{0.75}Co_{0.25}MoO_4$ follows the same catalytic behaviour as $NiMoO_4$ and $CoMoO_4$, $Ni_{0.25}Co_{0.75}MoO_4$ displays a totally opposite behaviour and $Ni_{0.5}Co_{0.5}MoO_4$ shows a minimum in propane conversion in the mixed Al_2O_3-MgO support.

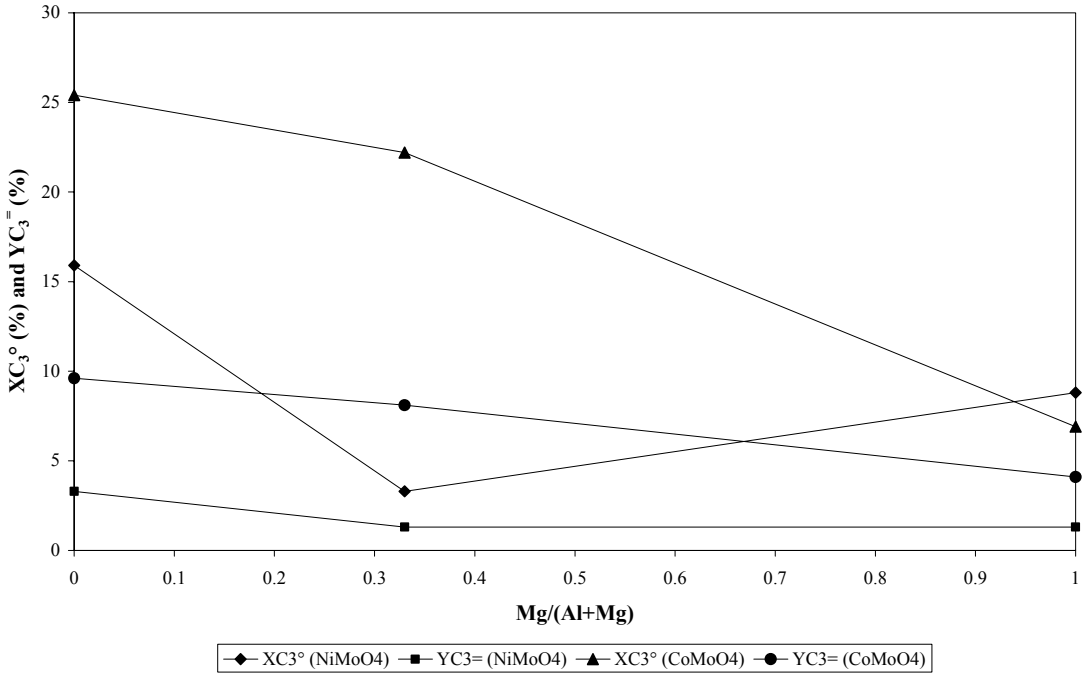

Fig.V.9: Evaluation of the catalytic performances of $NiMoO_4$ and $CoMoO_4$ prepared by the sol-gel method with respect to the amount of Mg included in the support (T = 753 K).

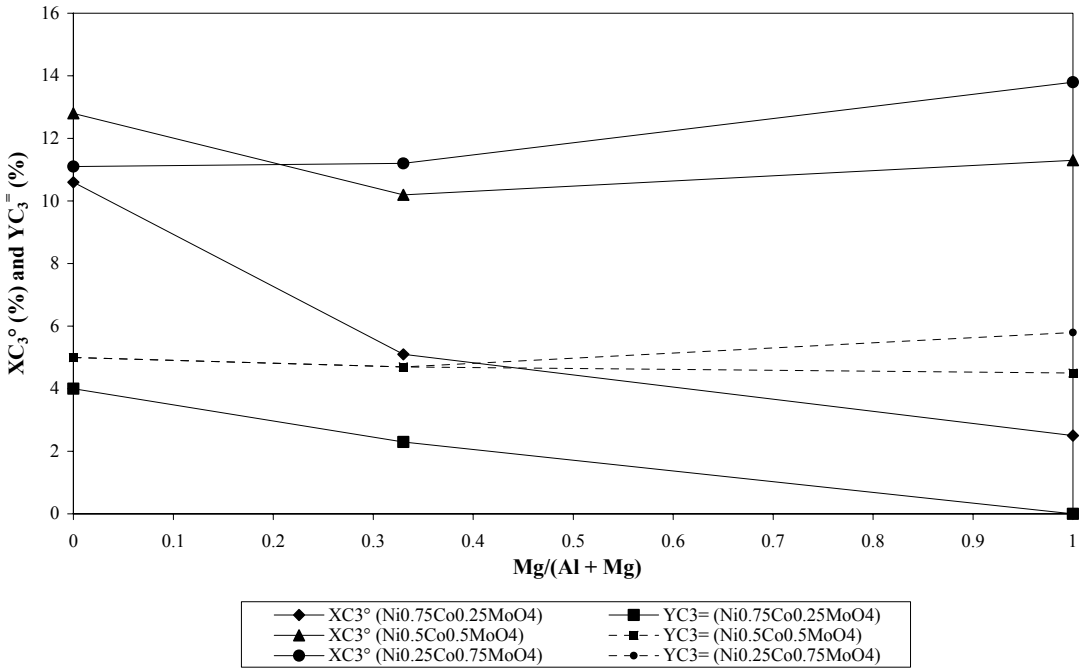

Fig.V.10: Evaluation of the catalytic performances of mixed Ni-Co molybdates prepared by the sol-gel method with respect to the amount of Mg included in the support (T = 753 K).

V.5 Al_2O_3-, MgO- and Al_2O_3-MgO-supported Ni and Co molybdates prepared by impregnation and sol-gel method

When Al_2O_3- or MgO-supported Ni and Co molybdates are prepared by sol-gel or impregnation method, the formation of analogous phases is observed, except in the case of the alumina-supported $NiMoO_4$ prepared by impregnation in which both α-phase and β-phase were detected. Sol-gel and impregnated catalysts are usually characterized by a different degree of cristallinity (higher in impregnated catalysts) and different peak intensities indicating preferential orientations.

Effect of the catalyst texture on the catalytic behaviour in alumina dispersed catalysts

Another way to explain the catalytic properties of alumina-supported catalysts is to look at the porous size of the solids. As already said, a pore characterized by a large diameter allows easily the access of the reactants to, and the departure of the products from, the active sites which are normally located in the pores.

For example, alumina-dispersed $CoMoO_4$ prepared by sol-gel and by impregnation method are characterized by an average pore diameter of 33.8 and 7.1 nm, respectively. The sol-gel prepared sample, which displays the higher catalytic activity is

the one with the largest pore diameter, allowing the reactant gases to easily enter inside the pore and reach the active sites. On the other hand, in the sample prepared by impregnation the active sites located in pores of small diameter are reached with more difficulties, leading to lower catalytic activity.

Correlation between catalytic activity and XPS analyses in magnesia-dispersed catalysts

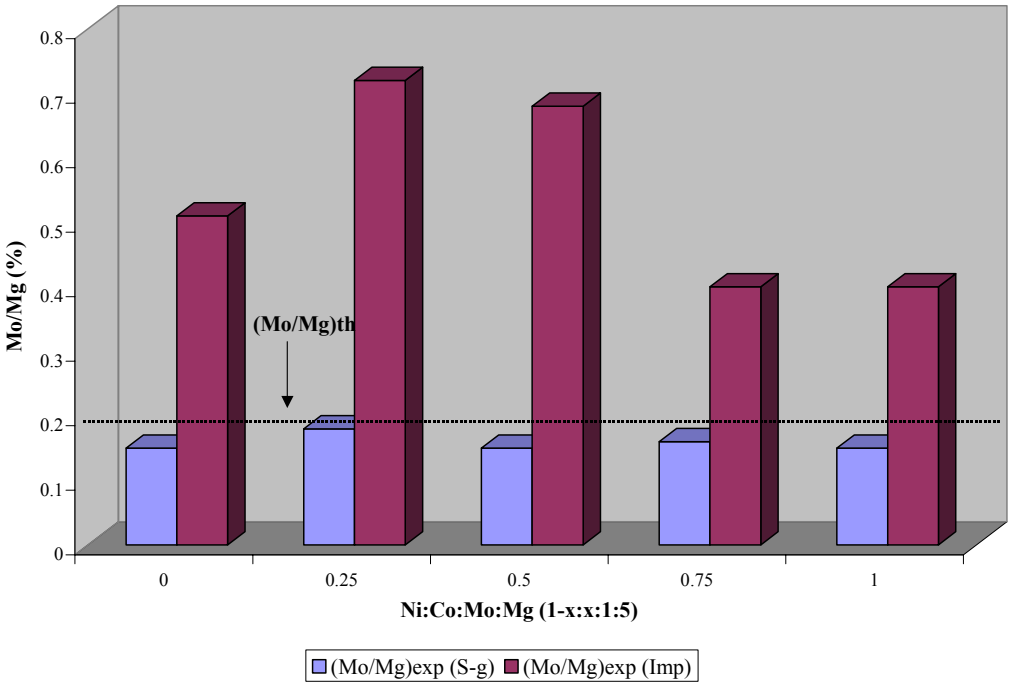

Fig.V.11: Experimental (Mo/Mg) atomic ratio in magnesia dispersed catalysts prepared by sol-gel and impregnation methods with respect to their composition.

Effect of the catalyst texture on the catalytic behaviour in magnesia dispersed catalysts

The average pore diameter of magnesia-supported $Ni_{1-x}Co_xMoO_4$ is normally higher if the sample is prepared by impregnation method (table III.6 in chapter III): but only in the case of the $CoMoO_4$ impregnated on MgO, its higher catalytic activity (making comparison with the analogous one prepared by sol-gel) could be explained by taking into account its higher pore diameter (20.8 and 31.7 nm for sol-gel and impregnated sample, respectively).

Correlation between catalytic activity and XPS analyses in mixed alumina-magnesia-dispersed catalysts

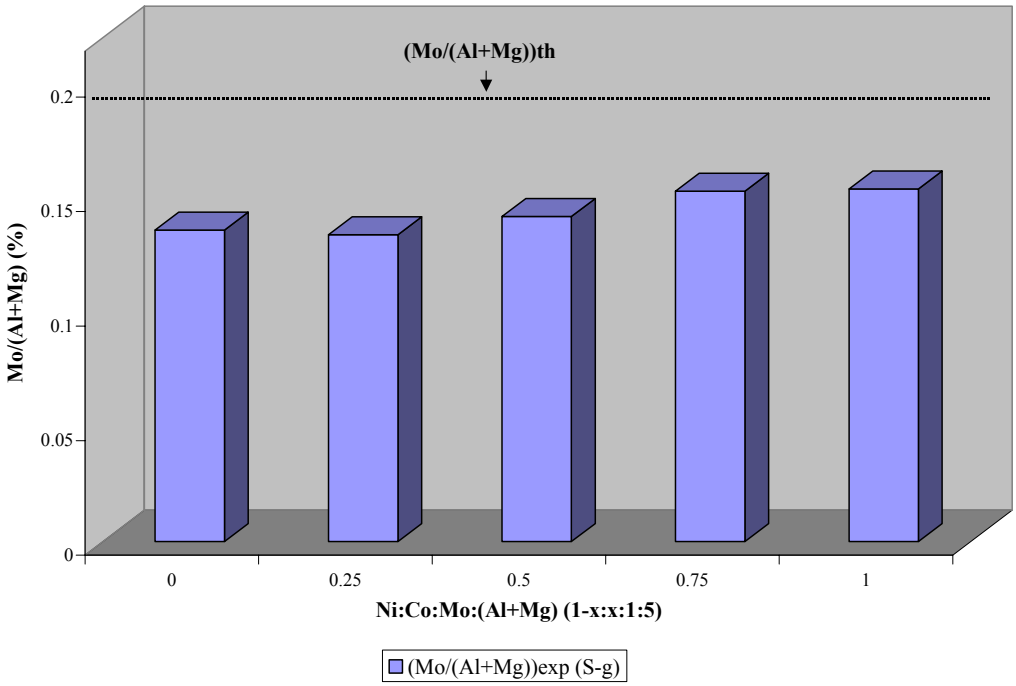

Fig.V.12: Experimental (Mo/(Al+Mg)) atomic ratio in mixed alumina-magnesia dispersed catalysts prepared by sol-gel method with respect to their composition.

Effect of the catalyst texture on the catalytic behaviour in mixed alumina-magnesia dispersed catalysts

The catalytic behavior of $Ni_{0.75}Co_{0.25}MoO_4$ catalyst supported on Al_2O_3 or Al_2O_3-MgO or MgO, seems to follow the idea that the higher the pore diameter, the higher the intrinsic propene yield (see table III.6, chapter III) .

V.6 TiO_2 and ZrO_2-supported Ni and Co molybdates prepared by impregnation

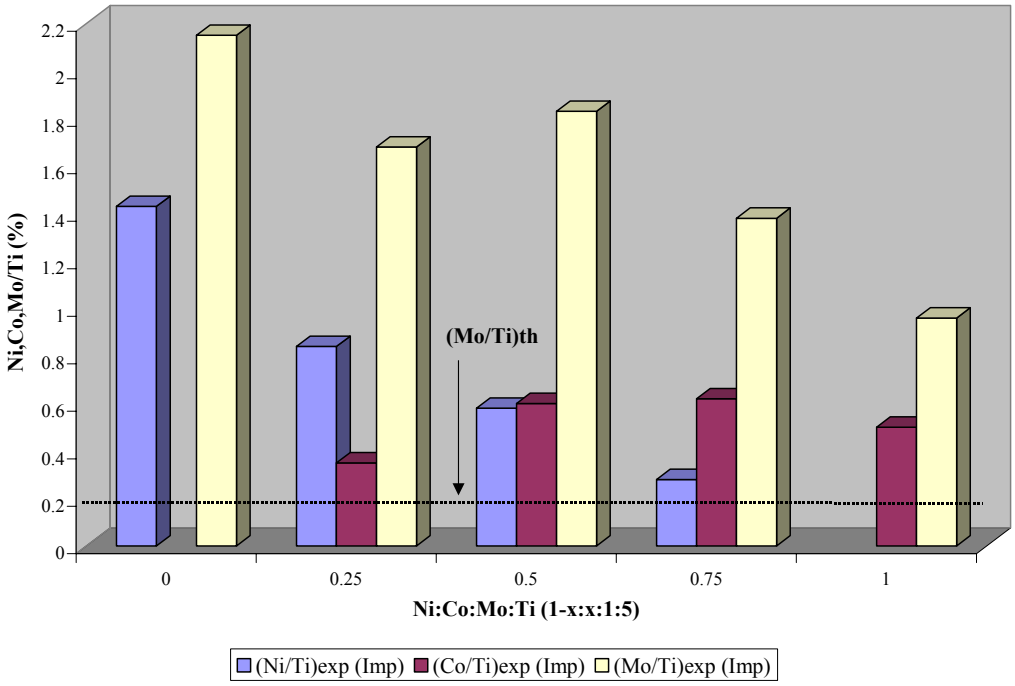

Fig.V.13: Experimental (Ni,Co,Mo/Ti) atomic ratios in titania supported catalysts with respect to their composition.

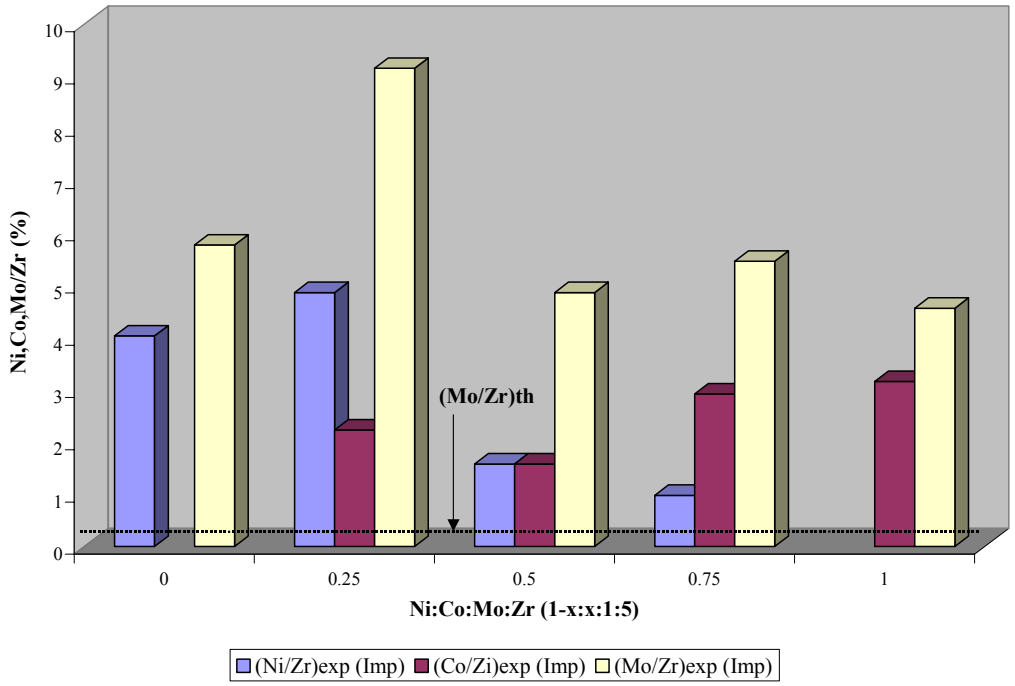

Fig.V.14: Experimental (Ni,Co,Mo/Zr) atomic ratios in zirconia supported catalysts with respect to their composition.